Proceedings of the Canadian Society for Mechanical Engineering International Congress
32nd Annual Conference of the Computational Fluid Dynamics Society of Canada
Canadian Society of Rheology Symposium
CSME-CFDSC-CSR 2025
May 25–28, 2025, Montréal, Québec, Canada

Fatigue damage constrained topology optimization for thermo-mechanical loading

Jinyu Gu[1,2], Yingjun Wang[1*], Hang Xu[2*]
[1] National Engineering Research Center of Novel Equipment for Polymer Processing, The Key Laboratory of Polymer Processing Engineering of the Ministry of Education, Guangdong Provincial Key Laboratory of Technique and Equipment for Macromolecular Advanced Manufacturing, South China University of Technology, Guangzhou 510641, China
[2] Department of Mechanical, Industrial and Aerospace Engineering, Concordia University, Montreal, QC H3A 0C3, Canada
*e-mail address: wangyj84@scut.edu.cn (Yingjun Wang), hang.xu@concordia.ca (Hang Xu)

Abstract—Structures in extreme thermal environments are vulnerable to fatigue damage under thermo-mechanical loads. To effectively address this issue via structural optimization design, this study proposes a thermo-mechanical fatigue damage-constrained topology optimization (TMFDCTO) method. This method aims to design lightweight structures while comprehensively accounting for the impact of thermo-mechanical-load-introduced fatigue damage. We first established a nonlinear fatigue damage analysis framework. This framework quantifies the effect of temperature variations on the S-N curve via the temperature-dependent Basquin equation. Morrow criterion then evaluates nonlinear fatigue damage caused by non-proportional thermo-mechanical loads. We formulated the analytical model of TMFDCTO by introducing a modified P-norm function to effectively process numerous constraints inherently existing in fatigue damage optimization. Finally, two numerical examples validated the feasibility and effectiveness of the proposed method.

Keywords-component; fatigue damage; thermo-mechanical loads; topology optimization; Morrow criterion

I. INTRODUCTION

Topology optimization (TO) is an advanced structural design methodology that determines optimal material distributions adhering to predefined constraints [1]. Over decades of development, robust TO examples in the literature include the solid isotropic material with penalization (SIMP) method, level-set method (LSM), evolutionary structural optimization (ESO) method, and the moving morphable components (MMC) or moving morphable voids (MMV) methods [2]. These methods have found increasing applications in different sectors, such as solid mechanics [3], thermal conduction [4], fluid dynamics [5], and acoustics [6]. However, further research is necessary to develop robust TO methods for fatigue performance in coupled physical fields, such as thermo-mechanical effects.

In extreme thermal environments, periodic temperature variations can lead to coupled thermo-mechanical effects in structures and cause undesired structural damage [7]. For instance, components of rocket engines, aircraft, and marine vessels usually operate in time-varying high-temperature conditions [8, 9]. High-temperature fluctuations deteriorate material properties, including but not limited to yield and fatigue strength, which eventually reduce components' durability. Moreover, cyclic temperature changes induce mismatches in thermal expansion and lead to thermal stress. This common and inevitable cyclic thermal-mechanical load causes fatigue failure, significantly impacting structural safety and decreasing operational lifespan. At present, there has not yet been a comprehensive investigation of the effects of thermo-mechanical coupling on fatigue damage within the TO framework, which creates an opportunity for further exploration to enhance the reliability and service life of structures.

To address this issue, this study integrates cyclic thermo-mechanical loading conditions into a TO framework to design lightweight structures with high fatigue life. The introduced framework gives rise to, for the first time, a thermo-mechanical fatigue damage-constrained topology optimization (TMFDCTO) method. Specifically, a fatigue analysis of the structure is conducted using a coupled thermo-mechanical finite element method (FEM). The Morrow criterion assesses structural fatigue damage, accounting for the nonlinear effects induced by non-proportional loading. A TO analytical model is then developed to minimize volume while meeting thermo-mechanical fatigue damage constraints. A modified P-Norm function effectively processes numerous constraints in fatigue damage TO. The sensitivity equation constraint function is derived and then the TMFDCTO model is solved by the Method of Moving Asymptotes (MMA) [10]. The model's effectiveness is demonstrated through two numerical examples.

This work has been supported by the Guangdong Basic and Applied Basic Re-search Foundation (grant No. 2024A1515011786) and Natural Sciences and Engineering Research Council of Canada for the financial support of the Discovery Grant (grant No. DGECR-2024-00078).

II. FATIGUE DAMAGE ANALYSIS UNDER THERMO-MECHANICAL LOADING

A. Thermo-mechanical coupling analysis

In the finite element analysis (FEA), the equilibrium equation for static elastic mechanics is formulated as follows:

$$\boldsymbol{F} = \boldsymbol{K}\boldsymbol{U} \tag{1}$$

where $\boldsymbol{F}$ is the load vector, $\boldsymbol{U}$ is the global displacement vector, and $\boldsymbol{K}$ is the global stiffness matrix.

In thermo-mechanical coupled analysis, mismatched thermal expansion in structures generates thermal-induced mechanical loads and causes thermal stresses. Therefore, when the structure is subjected to both mechanical load $\boldsymbol{F}^{\mathrm{m}}$ and thermo-mechanical load $\boldsymbol{F}^{\mathrm{th}}$, the resultant load $\boldsymbol{F}$ can be expressed as:

$$\begin{cases} \boldsymbol{F} = \boldsymbol{F}^{\mathrm{m}} + \boldsymbol{F}^{\mathrm{th}} \\ \boldsymbol{F}^{\mathrm{th}} = \sum_{e=1}^{Ne} \boldsymbol{F}_e^{\mathrm{th}} \\ \boldsymbol{F}_e^{\mathrm{th}} = \int_{\Omega_e} \boldsymbol{B}_e^{\mathrm{T}} \boldsymbol{D} \boldsymbol{\varepsilon}_e^{\mathrm{th}} d\Omega_e \end{cases} \tag{2}$$

The global thermo-mechanical load vector $\boldsymbol{F}^{\mathrm{th}}$ is assembled from the thermo-mechanical load vectors $\boldsymbol{F}_e^{\mathrm{th}}$ of individual elements. Here, $\boldsymbol{\varepsilon}_e^{\mathrm{th}}$ represents the thermal strain tensor. Considering the 2D plane stress condition and structures made of isotropic materials, its expression is given as:

$$\boldsymbol{\varepsilon}_e^{\mathrm{th}} = \alpha \Delta T_e \begin{bmatrix} 1 & 1 & 0 \end{bmatrix}^{\mathrm{T}} \tag{3}$$

where α denotes the coefficient of thermal expansion (CTE), and ΔT_e represents the difference between the element temperature T_e and the reference temperature T^{ref}.

The elastic equations of the elemental stress $\boldsymbol{\sigma}_e$ and von Mises stress σ_e^{vm} under external loading are as follows:

$$\boldsymbol{\sigma}_e = \boldsymbol{D}\boldsymbol{\varepsilon}_e = \boldsymbol{D}\boldsymbol{B}_e\boldsymbol{u}_e \tag{4}$$

$$\sigma_e^{vm} = \sqrt{\left(\sigma_{e,x}\right)^2 + \left(\sigma_{e,y}\right)^2 - \sigma_{e,x}\sigma_{e,y} + 3\tau_{e,xy}} \tag{5}$$

where $\boldsymbol{B}_e$ is the constitutive matrix of element e, $\boldsymbol{D}$ is the elasticity matrix, $\boldsymbol{\varepsilon}_e$ represents the strain tensor of element e, $\boldsymbol{u}_e$ denotes the nodal displacement of element e, and $\sigma_{e,x}$, $\sigma_{e,y}$, and $\tau_{e,xy}$ corresponds to the stress components of element e. In 2D, the expression for the elasticity matrix $\boldsymbol{D}$ is as follows:

$$\boldsymbol{D} = \frac{E_0}{1-\upsilon^2} \begin{bmatrix} 1 & \upsilon & 0 \\ & 1 & 0 \\ sym & & \dfrac{1-\upsilon}{2} \end{bmatrix} \tag{6}$$

where E_0 and υ represent the Young's modulus and Poisson's ratio of the material, respectively.

B. Nonlinear fatigue damage analysis

The counting of non-proportional cyclic loading is performed to assess the associated fatigue damage. This study employs the rainflow counting method for cycle counting of non-proportional loads. Therefore, the expressions for the stress amplitude $\sigma_{e,i}^a$ and mean stress $\sigma_{e,i}^m$ of cyclic load i at time t are as follows:

$$\begin{cases} \sigma_{e,i}^a = \dfrac{\left|\left(\sigma_{e,i}^{svm}(t)\right)_{\max} - \left(\sigma_{e,i}^{svm}(t)\right)_{\min}\right|}{2} \\ \sigma_{e,i}^m = \dfrac{\left(\sigma_{e,i}^{svm}(t)\right)_{\max} + \left(\sigma_{e,i}^{svm}(t)\right)_{\min}}{2} \end{cases} \tag{7}$$

where $\left(\sigma_{e,i}^{svm}(t)\right)_{\max}$ and $\left(\sigma_{e,i}^{svm}(t)\right)_{\min}$ are the maximum and minimum von Mises stresses during the i-th cyclic load at time t, respectively.

The equivalent stress amplitude is amended using the Morrow correction, which considers the influence of tensile stress on fatigue life. The amended expression is:

$$\bar{\sigma}_{e,i} = \sigma_{e,i}^a \left(1 - \frac{\max\left(\sigma_{e,i}^m, 0\right)}{\sigma_f'}\right)^{-1} \tag{8}$$

In addition, Basquin's equation at elevated temperatures was employed to account for the effect of temperature on fatigue life. The expression is as follows [11]:

$$\bar{\sigma}_{e,i} = \sigma_f' \left(2N_{f,e,i}\right)^b \left(T_e'\right)^c \tag{9}$$

where σ_f' is the fatigue strength coefficient, b is fatigue strength exponent of the material, $N_{f,e,i}$ is the number of ultimate fatigue cycles of element e under i-th cyclic load, T_e' is the absolute value of the elemental temperature in kelvin, and c is the temperature sensitivity parameter.

Under the effect of non-proportional cyclic loads, the fatigue damage of the structure accumulates nonlinearly. Morrow's criterion accounts for the interaction between loads, offering a more comprehensive approach [12]. Therefore, we apply

Morrow's rule to evaluate the fatigue damage of the structure, and the equation is as follows:

$$D_e = \sum_{i=1}^{NF} \frac{n_i}{N_{f,e,i}} \left(\frac{\bar{\sigma}_{e,i}}{\left(\bar{\sigma}_{e,i}\right)_{\max}} \right)^d \tag{10}$$

where D_e is the total damage of element e under multiple cyclic loads, $\bar{\sigma}_{e,i}$ is the stress amplitude, $\left(\bar{\sigma}_{e,i}\right)_{\max}$ is the maximum stress amplitude in the structural stress amplitude, n_i is the number of cycles of the stress amplitude $\bar{\sigma}_{e,i}$, d is the sensitivity index of the material to the history of variable amplitude stress, and $\left(\frac{\sigma_i}{\sigma_{\max}}\right)^d$ represents the influence of the maximum load in the loading spectrum on the damage caused by other loads.

III. THERMO-MECHANICAL FATIGUE TOPOLOGY OPTIMIZATION PROBLEM

A. TMFDCTO model

In this study, the TO problem aims to achieve a lightweight design under cyclic thermo-mechanical loading while satisfying fatigue damage constraints throughout the entire design domain. To achieve this, a TO model is developed to minimize the volume while satisfying the fatigue damage constraints. The mathematical representation of the model is as follows:

$$\begin{aligned} &\text{find}: \boldsymbol{\rho} \\ &\min: V(\boldsymbol{\rho}) = \sum_{e=1}^{NE} \rho_e v_e \\ &\text{s.t.} \begin{cases} \max\left(D_e\right) \le 1 \\ \boldsymbol{K}\boldsymbol{U} = \boldsymbol{F},\ \boldsymbol{F} = \boldsymbol{F}^{\mathrm{m}} + \boldsymbol{F}^{\mathrm{th}} \\ \boldsymbol{K}^{\mathrm{th}}\boldsymbol{T} = \boldsymbol{Q} \\ 0 < \rho_{\min} \le \rho_e \le 1,\ e = 1,2,\cdots,NE \end{cases} \end{aligned} \tag{11}$$

where $\boldsymbol{\rho}$ is the element density vector, NE represents the total number of elements in the structure, ρ_e denotes the relative density of the element e, v_e is the volume fraction of the initial design domain occupied by the element e, $\rho_{\min}$ is the lower density limit to avoid numerical singular values in FEA, and $\max\left(D_e\right)$ represents the maximum fatigue damage of the element. It is worth noting that the external thermal load is assumed to remain constant over time in this study.

B. Material interpolation scheme

In this study, the SIMP method is employed to interpolate both Young's modulus and thermal conductivity of the material. The corresponding expressions are as follows:

$$E\left(\rho_e\right) = E_{\min} + \left(\rho_e\right)^p \left(E_0 - E_{\min}\right) \tag{12}$$

$$\kappa\left(\rho_e\right) = \kappa_{\min} + \left(\rho_e\right)^{pk} \left(\kappa_0 - \kappa_{\min}\right) \tag{13}$$

Here, $E\left(\rho_e\right)$ and $\kappa\left(\rho_e\right)$ are the interpolated Young's modulus and thermal conductivity of element e, respectively. E_0 and κ_0 are the Young's modulus and thermal conductivity of the solid material, while $E_{\min}$ and $\kappa_{\min}$ are very small Young's moduli (commonly set to $10^{-9}E_0$) and thermal conductivity, typically used to represent void regions. p and pk are density penalty factors (typically equal to 3).

In addition, the thermo-mechanical load vector in Eq. (2) contains parameters $E\left(\rho_e\right)$ and $\alpha\left(\rho_e\right)$, which are both related to the material density. Since these two properties are density-dependent, they are combined into a single thermo-mechanical coefficient, denoted as $\psi\left(\rho_e\right)$. Therefore, the interpolation formula for the thermo-mechanical coefficient $\psi\left(\rho_e\right)$ is expressed as [13]:

$$\psi\left(\rho_e\right) = \left(E_{\min} + \left(\rho_e\right)^{pb}\left(E_0 - E_{\min}\right)\right)\alpha \tag{14}$$

C. Global fatigue damage constraint

To address the challenge posed by the large number of fatigue damage constraints in TO, we employ the P-norm function to manage these constraints effectively. The expression for the P-norm function applied to fatigue damage constraints is as follows:

$$D^{pn} = \left(\sum_{e=1}^{NE} \left(D_e\right)^{pn} \right)^{1/pn} \le 1 \tag{15}$$

where D^{pn} represents the fatigue damage calculated by the P-norm function, pn is the P-norm coefficient. Smaller pn values may result in inaccurate calculations, while larger pn values improve accuracy but can lead to instability in the optimization process. Therefore, following previous research [3], the pn value is set to 8 in this study.

Furthermore, the P-Norm function is refined to better approximate the maximum stress, as described in the literature [14]. This modification leverages scaling based on information from previous optimization iterations, effectively addressing the limitations of the P-Norm function in constraining maximum stress. The modified formulation is given as follows:

$$\bar{D}^{pn} = \chi^I D^{pn} \tag{16}$$

$$\chi^I = \gamma^I \frac{\max\left(\left(D_e\right)^{I-1}\right)}{\left(D^{pn}\right)^{I-1}} D^{pn} + \left(1-\gamma^I\right)\chi^{I-1}, \gamma^I \in (0,1] \quad (17)$$

where $\bar{D}^{pn}$ represents the fatigue damage calculated by the modified P-norm function, χ^I is the scaling factor for the I-th iteration, $\max\left(\left(D_e\right)^{I-1}\right)$ and $\left(D^{pn}\right)^{I-1}$ denote the maximum structural damage value and the P-norm value of structural damage for the (I-1)-th iteration, respectively. If oscillations, a value of $0 < \gamma^I < 1$ is selected; otherwise, $\gamma^I = 1$ is chosen. As the iteration converges, $\left(D^{pn}\right)^I \approx \left(D^{pn}\right)^{I-1}$ and $\max\left(\left(D_e\right)^I\right) \approx \max\left(\left(D_e\right)^{I-1}\right)$, thereby achieving convergence, i.e. $\chi^I D^{pn} \approx \max\left(\left(D_e\right)^I\right)$.

Meanwhile, fatigue optimization methods face challenges like those encountered in stress optimization, such as singular solutions and nonlinear behavior. Previous studies [15, 16] have demonstrated that employing a relaxation method to penalize Eq. (4) effectively addresses these issues. The equation for the aforementioned method is as follows:

$$\hat{\boldsymbol{\sigma}}_{e,i}(t) = \hat{\rho}_e^q \boldsymbol{D}_0 \boldsymbol{B}_e \boldsymbol{u}_{e,i}(t) \quad (18)$$

where $\hat{\boldsymbol{\sigma}}_{e,i}(t)$ represents the relaxed stress of an element at time t under the i-th cyclic load, q is the relaxation factor, with a typical value of 0.5.

IV. NUMERICAL EXAMPLES

This section evaluates the effectiveness of the proposed TMFDCTO method through a series of illustrative 2D examples, with the corresponding method flowchart presented in Fig. 1. Note that, structural fatigue typically occurs within the elastic range, below the material's yield stress, the material is assumed to remain elastic and isotropic throughout the analysis. In this study, Aluminum 7075 alloy (with material properties listed in TABLE I [11]) is used as an illustrative example for the optimization demonstrations. To ensure stable convergence, the move limit within the MMA algorithm is uniformly set to 0.01 across all examples. Additionally, the 2D design domains are discretized using a four-node quadrilateral, with an initial density of 1 uniformly assigned to all elements. The parameter settings related to the TMFDCTO method are detailed in TABLE II. All optimization examples are conducted on a desktop PC with an Intel® Core™ i7–13620H processor (2.4 GHz, 10 cores, 16 threads), 32 GB of RAM, and implemented using MATLAB® 2024b software.

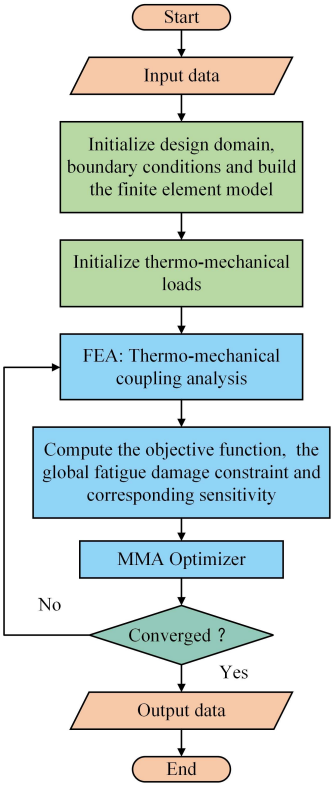

Figure 1. Flowchart of the presented TMFDCTO method

TABLE I. MECHANICAL AND THERMAL MATERIAL PROPERTIES

Material property	**Value**
Young's modulus E_0	71.7 GPa
Poisson's ratio υ	0.33
Fatigue strength coefficient σ_f'	1706.09 MPa
Fatigue strength exponent b	-0.1308
Sensitivity index of the material to the history of variable amplitude stress d	-0.45
Yield stress	508 MPa
Thermal conductivity κ_0	130 W/(m·K)
Coefficient of thermal expansion α	23.6×10^{-6} °C^{-1}
Reference temperature T^{ref}	25 °C

TABLE II. OPTIMIZATION PARAMETERS OF THE TMFDCTO METHOD

Parameter	**Value**
Density penalty factor p, pk, pb	3
Young's modulus for void element $E_{\min}$	$10^{-9}E_0$
Thermal conductivity for void element $\kappa_{\min}$	$10^{-9}\kappa_0$
2D plane thickness	10 mm
P-norm coefficient pn	8
Stress relaxation factor q	0.5
Filtering radius $r_{\min}$	2.5
Maximum iteration step	1000

A. *Simply supported structure*

In the first example, a simply supported structure is employed to illustrate the distinctions between the TMFDCTO method and the fatigue damage-constrained topology optimization (FDCTO) method, the latter of which does not incorporate thermos effects. The dimensions, boundary conditions, and loading configurations of the structure are shown in Fig. 2, and the entire structure is discretized into 5,000 elements. The history of non-proportional mechanical loads on the simply supported structures is depicted in Fig. 3. The number of load cycles is set to 10^7 for both types of mechanical loads, with a load width of $B = 6$ mm. The top boundary of the simply supported structure is subjected to a thermal load of $T = 60°C$, while the reference temperature at the bottom boundary is set to $T^{\text{ref}} = 25°C$.

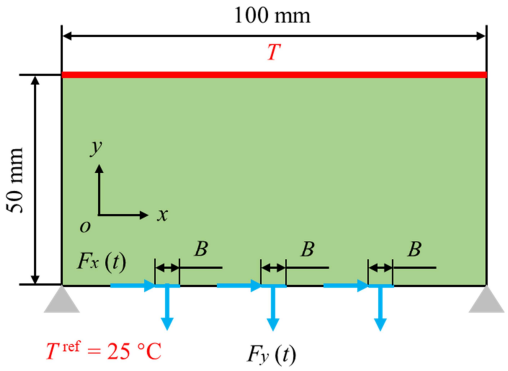

Figure 2. Design domain and boundary conditions of the simply supported structure

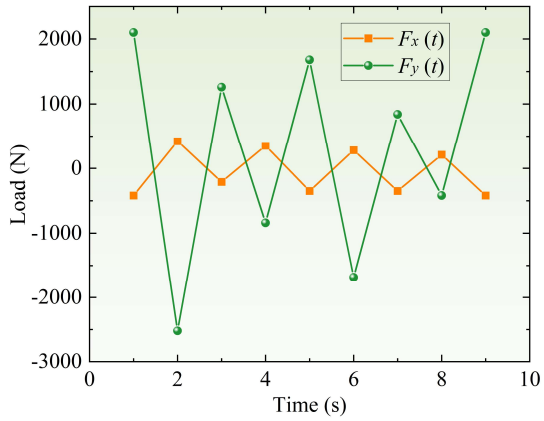

Figure 3. The history of mechanical loads on the simply supported structure

All parameter settings for the FDCTO method, which does not account for thermal loads, are identical to those used in the TMFDCTO method. TABLE III summarizes the optimization results for the simply supported structure. The results indicate that the two methods yield distinct topologies, both effectively constraining the maximum fatigue damage of the simply supported structure. The topology derived from the TMFDCTO method has a volume fraction (objective function) of 0.175, reflecting a 10.76% increase compared to the 0.158 volume fraction achieved by the FDCTO method. Additionally, the topology produced by the TMFDCTO method features thicker branches. This variation is attributed to the incorporation of thermal loads in the TMFDCTO method, which elevates the overall load acting on the structure. As a result, additional structural material is necessary to maintain fatigue resistance. These findings underscore the critical influence of considering thermal loads on the outcomes of fatigue-driven topology optimization.

TABLE III. THE OPTIMIZATION RESULTS OF THE SIMPLY SUPPORTED STRUCTURE

	TMFDCTO method	**FDCTO method**
Topology		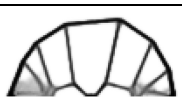
Damage	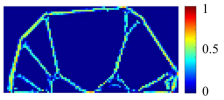	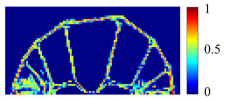
Temperature (°C)	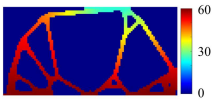	-
Objective	0.175	0.158
Max. damage	0.996	0.999
Max. stress	186.334 MPa	188.167 MPa

B. *Cantilever beam*

In the second example, a cantilever beam is utilized to examine the influence of varying thermal loads on the optimization results. The design domain, boundary conditions, and loading configurations of the cantilever beam are shown in Fig. 4. The structure is discretized into 5,000 finite elements for numerical analysis and optimization. The history of non-proportional mechanical loads on the cantilever beam is depicted in Fig. 5. Furthermore, the number of cycles for both mechanical loads is defined as 10^7, with the load width specified as $B = 2$ mm. The reference temperature at the top boundary of the cantilever beam is set to $T^{\text{ref}} = 25°C$, while varying thermal loads of $T = 60°C$, $90°C$, and $120°C$ are applied to the bottom boundary.

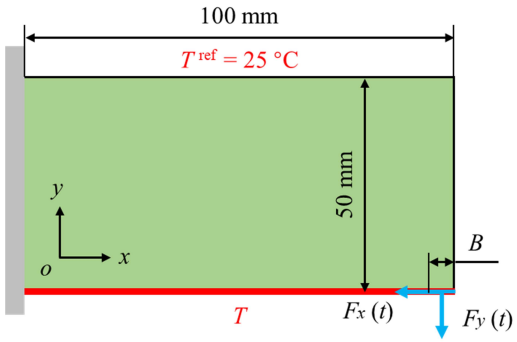

Figure 4. Design domain and boundary conditions of the cantilever beam

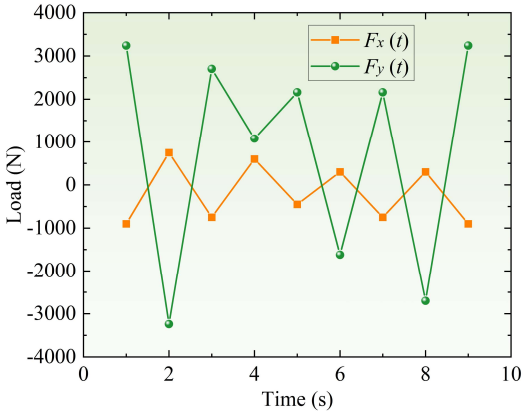

Figure 5. The history of mechanical loads on the cantilever beam

Fig. 6 depicts the optimized topology of the cantilever beam under different thermal loads. The results distinctly demonstrate substantial changes in the optimized topology in response to varying thermal loads. As the temperature increases from 60°C to 120°C, the regions in the topology with significant thermal influence shift downward This observation suggests that structural modifications are made to mitigate the effects of elevated temperatures on fatigue damage. Moreover, different mechanical loading conditions result in distinct optimization results.

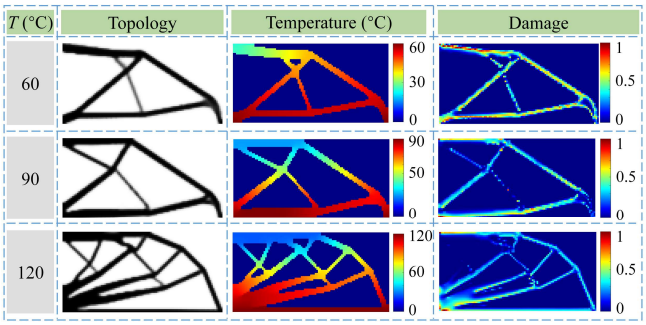

Figure 6. The optimization results of the cantilever beam

V. CONCLUSION

In this study, we presented a novel TO method to address nonlinear fatigue damage induced by thermo-mechanical loads. The proposed method employs the rainflow counting technique to evaluate stress levels resulting from non-proportional thermo-mechanical loads and incorporates the temperature-dependent Basquin equation to quantify the effects of temperature variations on fatigue life. The nonlinear Morrow criterion is adopted to comprehensively account for the impact of non-proportional loads on fatigue damage, while a modified P-Norm function is applied to accurately approximate the maximum fatigue damage. Example studies involving simply supported structures demonstrate the necessity of considering thermal loads in fatigue-constrained topology optimization.

ACKNOWLEDGMENT

This work has been supported by the Guangdong Basic and Applied Basic Re-search Foundation (grant No. 2024A1515011786) and Natural Sciences and Engineering Research Council of Canada for the financial support of the Discovery Grant (grant No. DGECR-2024-00078).

REFERENCES

[1] J.-H. Zhu, W.-H. Zhang, and L. Xia, "Topology optimization in aircraft and aerospace structures design," *Archives of Computational Methods in Engineering,* vol. 23, no. 4, pp. 595-622, 2015.

[2] Y. Wang, X. Li, K. Long, and P. Wei, "Open-source codes of topology optimization: a summary for beginners to start their research," *Computer Modeling in Engineering & Sciences,* vol. 137, no. 1, pp. 1-34, 2023.

[3] J. Gu, T. Gui, Q. Yuan, J. Qu, and Y. Wang, "Topology optimization method for local relative displacement difference minimization considering stress constraint," *Engineering Structures,* vol. 304, p. 117595, 2024.

[4] W. Sha, M. Xiao, Y. Wang, M. Huang, Q. Li, and L. Gao, "Topology optimization methods for thermal metamaterials: A review," *Int. J. Heat Mass Transfer,* vol. 227, p. 125588, 2024.

[5] G. Gao, J. Yang, X. Li, J. Gu, and Y. Wang, "Fluid topology optimization using quadtree-based scaled boundary finite element method," *Engineering Analysis with Boundary Elements,* vol. 169, p. 106019, 2024.

[6] G. Yan, X. Huang, Y. Li, W. Li, and S. Yao, "Three-field topology optimization of single-phase phononic crystals with desired bandgaps for elastic wave manipulation," *Engineering Structures,* vol. 326, p. 119554, 2025.

[7] J.-Y. Jeong, S.-J. Park, D.-C. Ahn, J.-M. Lee, M.-W. Lee, and Y.-J. Kim, "Thermo-mechanical fatigue analysis of ferritic stainless steel STS444LM for exhaust manifold application," *Engineering Failure Analysis,* vol. 167, p. 108916, 2025.

[8] V. Gray, J. P. Jones, M. T. Whittaker, R. J. Lancaster, C. J. Pretty, and S. J. Williams, "A holistic approach to Thermo-Mechanical Fatigue phase angle effects for an aerospace nickel superalloy," *International Journal of Fatigue,* vol. 156, p. 106631, 2022.

[9] C. Qian *et al.*, "Life prediction based on fatigue-environment damage under multiaxial thermo-mechanical loading," *Eng. Fract. Mech.,* vol. 308, p. 110357, 2024.

[10] K.-T. Zuo, L.-P. Chen, Y.-Q. Zhang, and J. Yang, "Study of key algorithms in topology optimization," *The International Journal of Advanced Manufacturing Technology,* vol. 32, no. 7-8, pp. 787-796, 2006.

[11] E. Z. Fadhel, "Effect of the elevated temperature on fatigue behavior of aluminum alloy AA 7075," *J. Univ. Babylon Eng. Sci.,* vol. 26, no. 8, pp. 256-264, 2018.

[12] R. G. Lambert, "Plastic Work Interaction Damage Rule Applied to Narrow-Band Gaussian Random Stress Situations," *ASME. Journal of Pressure Vessel Technology,* vol. 110, no. 1, pp. 88-90, 1988.

[13] T. Gao and W. Zhang, "Topology optimization involving thermo-elastic stress loads," *Structural and Multidisciplinary Optimization,* vol. 42, no. 5, pp. 725-738, 2010.

[14] C. Le, J. Norato, T. Bruns, C. Ha, and D. Tortorelli, "Stress-based topology optimization for continua," *Structural and Multidisciplinary Optimization,* vol. 41, no. 4, pp. 605-620, 2009.

[15] M. Kočvara and M. Stingl, "Solving stress constrained problems in topology and material optimization," *Structural and Multidisciplinary Optimization,* vol. 46, no. 1, pp. 1-15, 2012.

[16] E. Holmberg, B. Torstenfelt, and A. Klarbring, "Stress constrained topology optimization," *Structural and Multidisciplinary Optimization,* vol. 48, no. 1, pp. 33-47, 2013.